

Analysing powers for the reaction $np \rightarrow pp\pi^-$ and for np elastic scattering from 270 to 570 MeV

M. Daum², M. Finger^{3,4}, M. Finger, Jr.⁴, J. Franz¹, F.H. Heinsius¹, A. Janata⁴, K. Königsmann¹, H. Lacker^{*1}, F. Lehar⁵, H. Schmitt¹, W. Schweiger¹, P. Sereni¹, and M. Slunečka^{3,4}

¹ Fakultät für Physik der Universität Freiburg, D-79104 Freiburg, Fed. Rep. Germany

² PSI, Paul-Scherrer-Institut, CH-5232 Villigen, Switzerland

³ Charles University, Faculty of Mathematics and Physics, V Holešovičkách 2, CZ-18000 Praha 8, Czech Republic

⁴ Joint Institute for Nuclear Research, LNP, RU-141980 Dubna, Moscow Region, Russia

⁵ DAPNIA/SPP, CEA/Saclay, F-91191 Gif-sur-Yvette CEDEX, France

Received: YYYY ?, 2001 / Accepted: XXXX ?, 2001

Abstract. The analysing power of the reaction $np \rightarrow pp\pi^-$ for neutron energies between threshold and 570 MeV has been determined using a transversely polarised neutron beam at PSI. The reaction has been studied in a kinematically complete measurement using a time-of-flight spectrometer with large acceptance. Analysing powers have been determined as a function of the c.m. pion angle in different regions of the proton-proton invariant mass. They are compared to other data from the reactions $np \rightarrow pp\pi^-$ and $pp \rightarrow pp\pi^0$. The np elastic scattering analysing power was determined as a by-product of the measurements.

1 Introduction

Single pion production is the main inelastic hadronic process in nucleon-nucleon collisions for beam energies below 1 GeV. During the last decade, new results have been obtained for proton-proton induced reactions. The new data, taken at proton cooler synchrotrons, triggered new theoretical efforts. However, a complete understanding of the various production mechanisms requires high quality data in all possible pion production reactions. In this paper, we report on measurements of the spin dependence in the reaction $np \rightarrow pp\pi^-$ and in the elastic np scattering.

1.1 Pion production in neutron proton collisions

Assuming isospin invariance in strong interactions, all single pion production reactions in nucleon-nucleon collisions with three body final states can be decomposed into three partial cross sections $\sigma_{I_i I_f}$ [1]. Here, I_i and I_f denote the isospin of the nucleon-nucleon system in the initial and final state. Information on the isoscalar cross section σ_{01} can be obtained by comparing charged pion production in neutron-proton collisions with the reaction $pp \rightarrow pp\pi^0$ [2].

The production mechanism is often discussed in terms of partial waves. In this paper, the notation

$${}^{2S+1}L_J \rightarrow {}^{2S'+1}L'_J, \ell_J$$

Correspondence to: lacker@lal.in2p3.fr

is adopted, where S is the total spin, L the orbital angular momentum and J the total angular momentum of the two nucleons in the initial state, while S' , L' and J' give the corresponding angular momenta in the final state. The orbital angular momentum of the pion with respect to the final state nucleon-nucleon system is denoted ℓ .

Partial waves with a relative angular momentum $L = 0$ for the proton-proton final state play a particular role due to the strong final state interaction at small relative momenta. Amongst the partial waves with $pp({}^1S_0)$ final states, ${}^3P_0 \rightarrow {}^1S_0s_0$, ${}^3P_2 \rightarrow {}^1S_0d_2$ and ${}^3F_2 \rightarrow {}^1S_0d_2$ contribute to σ_{11} , whereas ${}^3D_1 \rightarrow {}^1S_0p_1$ and ${}^3S_1 \rightarrow {}^1S_0p_1$ contribute to σ_{01} . Effects from these partial waves are enhanced if the phase space is restricted to small proton-proton invariant masses.

1.2 Former Experiments

For a long time, the experimental knowledge on the reaction $np \rightarrow NN\pi^\pm$ was rather weak. Many observables, e.g., invariant mass or angular distributions, as well as integrated cross sections were not very well known [3,4,5,6,7,8,9,10,11,12]. As a consequence, no conclusive result concerning the size and the role of the cross section σ_{01} has been found, see e.g. Refs. [13,14]. In ref. [13] one strictly assumes isospin invariance, whereas in ref. [14] one compares the results of this assumption with the calculations, where np inelastic one-pion-production reactions are considered to be independent of each other. For a discussion of the partly contradictory experimental results for the reactions $np \rightarrow NN\pi^\pm$ and $pp \rightarrow pp\pi^0$ see also Ref. [2].

During the last decade, new medium energy accelerators provided secondary neutron beams of high intensity and polarisation. This resulted in a substantial improvement of the experimental situation. Single spin observables for the reaction $np \rightarrow pp\pi^-$ have been measured at TRIUMF at 443 MeV [12] and at SATURNE at 572, 784, 1012 and 1134 MeV [15]. Exclusive experiments were performed at TRIUMF, with proton beam energies of 353, 403 and 440 MeV incident on a deuterium target [16,17]. Events with small proton-proton invariant masses were selected to investigate partial wave contributions with a $pp(^1S_0)$ final state. The results showed the significance of the σ_{01} cross section in that particular phase space configuration. A partial wave analysis considering $^3S_1 \rightarrow ^1S_0p_1$ and $^3D_1 \rightarrow ^1S_0p_1$ for the $I = 0$ and $^3P_0 \rightarrow ^1S_0s_0$ for the $I = 1$ initial state was performed [17]. At 440 MeV, a small contribution from pion d-waves, $^3P_2 \rightarrow ^1S_0d_2$ and $^3F_2 \rightarrow ^1S_0d_2$, has been reported [17].

Recently, differential and integrated cross sections for the reaction $np \rightarrow pp\pi^-$ between threshold and 570 MeV have been measured at PSI [2]. All observables revealed a significant contribution of σ_{01} . An enhancement in the proton-proton invariant mass distribution was observed at small values in agreement with the expected signal from Sp partial waves. In addition, large anisotropies and forward-backward asymmetries in the pion angular distributions were observed which was interpreted as a strong contribution of partial waves with Sp final states. From the measurement of the $np \rightarrow pp\pi^-$ cross section, σ_{01} was obtained using existing $pp \rightarrow pp\pi^0$ data [18,19,20,21,22]. It was found to be of the same order as σ_{11} in the energy range between 315 MeV and 400 MeV. The excitation function of σ_{01} is reasonably described by a function $\propto \eta^4$, where $\eta = p_{\pi,\max}^*/m_{\pi^+}$ is the maximum value of the dimensionless c.m. pion momentum. This dependence is expected if σ_{01} is carried by Sp partial waves.

Within the above mentioned PSI experiment [2] also spin dependent observables of the reaction $np \rightarrow pp\pi^-$ have been measured and are presented in this paper.

Spin dependent observables are very sensitive to the interference between amplitudes from the $I = 0$ and $I = 1$ initial state. Hence, the measurement of spin observables for the reactions $np \rightarrow pp\pi^-$ and $pp \rightarrow pp\pi^0$ can provide additional information on σ_{01} .

2 Experiment

The experiment was performed at the Paul-Scherrer-Institut (PSI). The set-up and the analysis are described in more detail elsewhere [2,23]. Data were taken with a transversely polarised neutron beam with about 50 % of the data measured with horizontal and about 50 % with vertical polarisation. To minimize detector induced asymmetries, the polarisation of the primary proton beam was reversed every second.

The proton beam polarisation was monitored by measuring the rate asymmetry between both polarisation directions for protons elastically scattered on a thin Carbon

target [24]. The energy dependent neutron beam polarisation was measured in a former experiment [25].

Two beam monitors [24] were used to record continuously the polarised neutron beam properties during data taking. This information was used in the off-line analysis to check possible drifts of the beam polarisation and for eventual intensity and position differences for the two polarisation directions.

For the kinematically complete measurement of the reaction $np \rightarrow pp\pi^-$, a time-of-flight (TOF) spectrometer with large angular and momentum acceptance was used. It consisted of a liquid hydrogen target, two drift chamber stacks together with a two dimensional scintillator hodoscope and a 3×3 m² TOF wall. Events were selected by requiring at least two hits in the hodoscope, at least one hit in the TOF wall and hits in the first drift chamber. In addition, events fulfilling a minimum bias trigger were selected with a prescaling factor to study elastic scattering events. The experiment relied on the measurement of the energy for the incident neutron and the emission angles and velocities of at least two of the three charged particles in the final state. The energy of each incident neutron was determined from a TOF measurement along a 20 m long flightpath using the 50 MHz time structure of the neutron beam. The reaction $np \rightarrow pp\pi^-$ was reconstructed using a kinematical fit technique. Background from the target surroundings in the final data sample was measured with an empty target cell and was found to be between 8 % at 315 MeV and 4 % at 550 MeV. Monte Carlo simulation studies showed that background from other reactions in the liquid hydrogen target were negligible. For details of the event identification, see ref. [2].

3 Determination of analysing powers

For a given neutron energy T_n , the following basis in the c.m. system of the reaction $np \rightarrow pp\pi^-$, $\{\mathbf{S}, \mathbf{N}, \mathbf{L}\}$, is chosen: The unit vector \mathbf{L} is defined by the neutron momentum in the c.m. system $\mathbf{L} = \mathbf{p}_n^*/|\mathbf{p}_n^*|$; \mathbf{N} is the vector normal to the reaction plane defined by $\mathbf{N} = (\mathbf{p}_n^* \times \mathbf{p}_\pi^*)/|\mathbf{p}_n^* \times \mathbf{p}_\pi^*|$; \mathbf{S} is chosen such that a right-handed orthonormal system is obtained. In the present experiment, the neutron beam is polarised, the target is not polarised and the polarisation of the final state protons is not analysed. In this case, the spin dependent cross section $d\sigma$ reads

$$d\sigma = d\sigma_0 \cdot (1 + P_S \cdot A_{S0} + P_N \cdot A_{N0} + P_L \cdot A_{L0}) \quad (1)$$

where $d\sigma_0$ is the spin-averaged differential cross section and P_S , P_N and P_L are the projections of the beam polarisation vector \mathbf{P} onto the three basis vectors \mathbf{S} , \mathbf{N} and \mathbf{L} . The observables A_{S0} , A_{N0} and A_{L0} are called (beam) analysing powers.

For a fixed neutron energy, the cross section $d\sigma$ is a function of five independent kinematical variables in the final state. Integrating over all phase space variables except the proton-proton invariant mass M_{pp} , the pion c.m. angle θ_π^*

and the angle ϕ between \mathbf{N} and \mathbf{P} , one obtains for a transversely polarised neutron beam

$$d\sigma(T_n, M_{pp}, \theta_\pi^*, \phi) = d\sigma_0(T_n, M_{pp}, \theta_\pi^*) \cdot (1 + P(T_n) \cdot A_{S0}(T_n, M_{pp}, \theta_\pi^*) \cdot \sin \phi + P(T_n) \cdot A_{N0}(T_n, M_{pp}, \theta_\pi^*) \cdot \cos \phi), \quad (2)$$

since the longitudinal polarisation component vanishes, $P_L = 0$.

The analysing powers A_{N0} and A_{S0} were determined using the method of weighted sums [26] which assumes an azimuthal symmetry of the detector around the beam axis. The assumption of parity conservation in strong interactions implies $A_{S0}(M_{pp}, \theta_\pi^*) = 0$. Hence, the measurement of A_{S0} provides an important cross-check for the analysis.

The beam polarisation depends on the neutron energy [25]. It was taken into account in the analysis by weighting each event i with the beam polarisation value $P_i = P(T_n)$ at the measured neutron energy T_n . The reconstruction efficiency $a_{pp\pi^-}$ shows a strong dependence on the kinematical variable θ_π^* and in particular on M_{pp} [2, 23]. For very small M_{pp} values, both proton tracks are close together and the efficiency drops. As a consequence, each event was additionally weighted by the inverse of the reconstruction efficiency, $a_{pp\pi^-}^{-1}(M_{pp}, \theta_\pi^*)$. This results in the following matrix equation for the estimators of the analysing powers A_{N0} and A_{S0} :

$$\begin{pmatrix} \sum a_i^{-1} P_i \cos \phi_i \\ \sum a_i^{-1} P_i \sin \phi_i \end{pmatrix} = \begin{pmatrix} \sum a_i^{-1} P_i^2 \cos^2 \phi_i & \sum a_i^{-1} P_i^2 \sin \phi_i \cos \phi_i \\ \sum a_i^{-1} P_i^2 \sin \phi_i \cos \phi_i & \sum a_i^{-1} P_i^2 \sin^2 \phi_i \end{pmatrix} \begin{pmatrix} A_{N0} \\ A_{S0} \end{pmatrix} \quad (3)$$

where the index i runs over all events passing the reconstruction cuts.

4 Results and discussion

4.1 Elastic scattering $np \rightarrow np$

As a by-product, analysing powers for the np elastic scattering, using events from the minimum bias trigger sample, have been measured. Adopting the convention of Ref. [27], the analysing powers of interest for elastic scattering are denoted A_{00n0} and A_{00s0} . They correspond to A_{N0} and A_{S0} by replacing \mathbf{p}_π^* with the momentum vector of the scattered neutron \mathbf{p}_n^* . For elastic scattering, there is only one independent kinematic variable in the final state. As a consequence, the weighting of the events by the reconstruction efficiency was omitted in (3).

For the determination of the analysing powers, the data with neutron energies between 270 and 570 MeV were subdivided in 10 bins of equal width. For each neutron energy bin, the mean neutron energy was computed. The analysing powers A_{00n0} and A_{00s0} were calculated as a function of the neutron c.m. scattering angle θ_n^* . The results for A_{00n0} are shown in Fig. 1. The numerical values are given in Tab. 1.

A contribution to the systematic uncertainty is the error on the neutron beam polarisation of about 3 %. Background contributions from the target surroundings and drift chamber materials were determined from runs with an empty target cell and found to be 12 % averaged over the considered neutron energies. The spin dependent asymmetry from this background source showed similar results as the data with the full target cell. However, these asymmetries were determined with much less statistical precision. Under the assumption that the asymmetry from this background differs by ± 20 % from the asymmetry of signal events, the relative systematic error was estimated to be ± 2 %. Inelastic reactions in the liquid hydrogen target gave only a small contribution of 3 % at 270 MeV and 1 % at 550 MeV the asymmetry of which could not be determined. Under the conservative assumption that the analysing power of this background can take any value between +1 and -1, an additional systematic error was assigned which reads ± 3 % at 270 MeV and 1 % at 550 MeV. All systematic error contributions were added in quadrature.

As can be seen from Fig. 1, the analysing powers A_{00n0} are in good agreement with the results of a partial wave analysis performed by Arndt et al. [28] where the new data have not been taken into account. The analysing powers A_{00s0} for the different neutron energy bins are consistent with zero as it is expected due to parity conservation [23].

Under the assumption of parity conservation, the ratio A_{00s0}/A_{00n0} allows to test if the horizontally (vertically) polarised beam contained additional, small polarisation components in the vertical (horizontal) direction. For all neutron energies, this ratio was found to be consistent with zero within the statistical uncertainties. Averaging over all neutron energies, an asymmetry

$$\langle \epsilon_s \rangle = \langle P \rangle \cdot \langle A_{00s0} \rangle = -0.0002 \pm 0.001$$

was found. This has to be compared to the energy averaged asymmetry

$$\langle \epsilon_n \rangle = \langle P \rangle \cdot \langle A_{00n0} \rangle = 0.05 \pm 0.001.$$

Hence, the relative contribution of a transverse component perpendicular to the main transverse polarisation was smaller than 3% at 68% confidence level. This finding is in agreement with the asymmetries determined from the beam monitor scaler rates.

4.2 Analysing powers for $np \rightarrow pp\pi^-$

For the determination of the analysing powers for the reaction $np \rightarrow pp\pi^-$, the data were subdivided in nine neutron energy bins where the first bin was between threshold and 330 MeV while the other bins were of 30 MeV width. For each neutron energy bin, the mean neutron energy was calculated from the neutron energy distribution. The results are presented as a function of $\cos \theta_\pi^*$.

In general, statistical errors are the main uncertainties. With increasing neutron energy, the statistical error decreases and the systematic error becomes more and more

T_n	θ_n^*	A_{00n0}	σ_{stat}	σ_{sys}	T_n	θ_n^*	A_{00n0}	σ_{stat}	σ_{sys}	T_n	θ_n^*	A_{00n0}	σ_{stat}	σ_{sys}
284	113.0	-0.108	0.111	0.005	404	112.9	-0.448	0.077	0.019	496	112.9	-0.321	0.075	0.013
	117.8	-0.194	0.070	0.009		117.8	-0.318	0.052	0.013		117.8	-0.317	0.053	0.012
	122.8	-0.119	0.048	0.006		122.8	-0.125	0.037	0.005		122.7	-0.234	0.039	0.009
	127.6	-0.125	0.039	0.006		127.5	-0.151	0.031	0.006		127.5	-0.171	0.035	0.007
	132.5	-0.106	0.037	0.005		132.5	-0.191	0.030	0.008		132.6	-0.142	0.033	0.006
	137.5	-0.137	0.036	0.006		137.5	-0.138	0.029	0.006		137.5	-0.136	0.031	0.005
	142.5	-0.095	0.037	0.004		142.5	-0.116	0.028	0.005		142.5	-0.156	0.031	0.006
	147.5	-0.133	0.038	0.006		147.5	-0.074	0.029	0.003		147.5	-0.142	0.031	0.006
	152.5	-0.137	0.039	0.006		152.5	-0.108	0.030	0.005		152.5	-0.100	0.031	0.004
	157.4	-0.075	0.041	0.004		157.5	-0.091	0.032	0.004		157.4	-0.103	0.034	0.004
	162.4	-0.003	0.046	0.002		162.4	-0.069	0.037	0.003		162.3	-0.040	0.039	0.002
	167.1	-0.074	0.062	0.004		167.2	-0.033	0.050	0.001		167.1	-0.029	0.053	0.001
	171.9	0.041	0.112	0.002		171.8	-0.029	0.088	0.001		171.8	-0.094	0.095	0.004
	176.3	-0.260	0.370	0.012		176.4	0.041	0.277	0.017		176.3	-0.133	0.285	0.005
314	113.0	-0.057	0.096	0.003	435	112.9	-0.178	0.072	0.007	525	112.8	-0.338	0.055	0.013
	117.8	-0.334	0.062	0.016		117.8	-0.291	0.049	0.011		117.8	-0.354	0.038	0.013
	122.8	-0.104	0.042	0.005		122.8	-0.224	0.035	0.008		122.7	-0.173	0.028	0.006
	127.6	-0.204	0.034	0.010		127.5	-0.206	0.031	0.008		127.5	-0.234	0.025	0.009
	132.5	-0.137	0.033	0.006		132.6	-0.142	0.029	0.005		132.5	-0.148	0.024	0.006
	137.5	-0.149	0.032	0.007		137.5	-0.126	0.028	0.005		137.5	-0.145	0.023	0.005
	142.5	-0.104	0.032	0.005		142.5	-0.153	0.028	0.006		142.5	-0.111	0.022	0.004
	147.5	-0.103	0.033	0.005		147.5	-0.144	0.028	0.005		147.5	-0.108	0.023	0.004
	152.5	-0.071	0.034	0.003		152.5	-0.150	0.029	0.006		152.5	-0.055	0.023	0.002
	157.4	-0.085	0.036	0.004		157.4	-0.081	0.031	0.003		157.4	-0.103	0.024	0.004
	162.4	-0.089	0.041	0.004		162.3	-0.019	0.036	0.001		162.3	-0.069	0.029	0.003
	167.1	-0.093	0.055	0.004		167.1	-0.059	0.048	0.002		167.1	-0.075	0.039	0.003
	171.9	0.076	0.100	0.004		171.9	-0.218	0.084	0.008		171.9	-0.010	0.069	0.000
	176.3	-0.110	0.309	0.005		177.3	-0.315	0.241	0.012		176.3	-0.336	0.196	0.013
344	113.0	-0.306	0.084	0.013	465	112.9	-0.151	0.076	0.006	550	112.9	-0.284	0.063	0.011
	117.8	-0.207	0.056	0.009		117.8	-0.289	0.052	0.011		117.8	-0.229	0.044	0.009
	122.8	-0.182	0.039	0.008		122.7	-0.279	0.038	0.011		122.7	-0.194	0.034	0.007
	127.6	-0.184	0.032	0.008		127.6	-0.189	0.033	0.007		127.6	-0.216	0.031	0.008
	132.5	-0.146	0.031	0.006		132.5	-0.166	0.031	0.006		132.6	-0.200	0.029	0.008
	137.5	-0.194	0.031	0.009		137.5	-0.107	0.030	0.004		137.5	-0.157	0.028	0.006
	142.5	-0.147	0.030	0.007		142.5	-0.141	0.029	0.006		142.5	-0.103	0.027	0.004
	147.5	-0.161	0.031	0.007		147.5	-0.137	0.030	0.005		147.5	-0.068	0.027	0.003
	152.5	-0.033	0.032	0.002		152.5	-0.079	0.031	0.003		152.5	-0.087	0.028	0.003
	157.4	-0.172	0.034	0.008		157.4	-0.096	0.033	0.004		157.4	-0.099	0.030	0.004
	162.3	-0.090	0.038	0.004		162.3	-0.088	0.038	0.003		162.3	-0.094	0.034	0.004
	167.1	-0.033	0.052	0.002		167.1	-0.005	0.052	0.000		167.1	0.013	0.048	0.001
	171.8	0.020	0.094	0.001		171.8	-0.170	0.091	0.007		171.9	-0.104	0.086	0.004
	176.3	0.227	0.292	0.010		176.5	-0.334	0.293	0.013		176.3	-0.333	0.243	0.013
374	112.9	-0.237	0.081	0.010										
	117.8	-0.355	0.054	0.016										
	122.8	-0.199	0.038	0.009										
	127.6	-0.141	0.032	0.006										
	132.5	-0.123	0.030	0.005										
	137.5	-0.176	0.030	0.008										
	142.5	-0.124	0.029	0.005										
	147.5	-0.104	0.030	0.005										
	152.5	-0.115	0.031	0.005										
	157.5	-0.128	0.032	0.006										
	162.5	-0.063	0.037	0.003										
	167.5	-0.101	0.051	0.004										
	172.5	0.039	0.090	0.002										
	177.5	0.644	0.286	0.028										

Table 1. Analysing powers A_{00n0} for the np elastic scattering. Quoted are statistical and systematic errors.

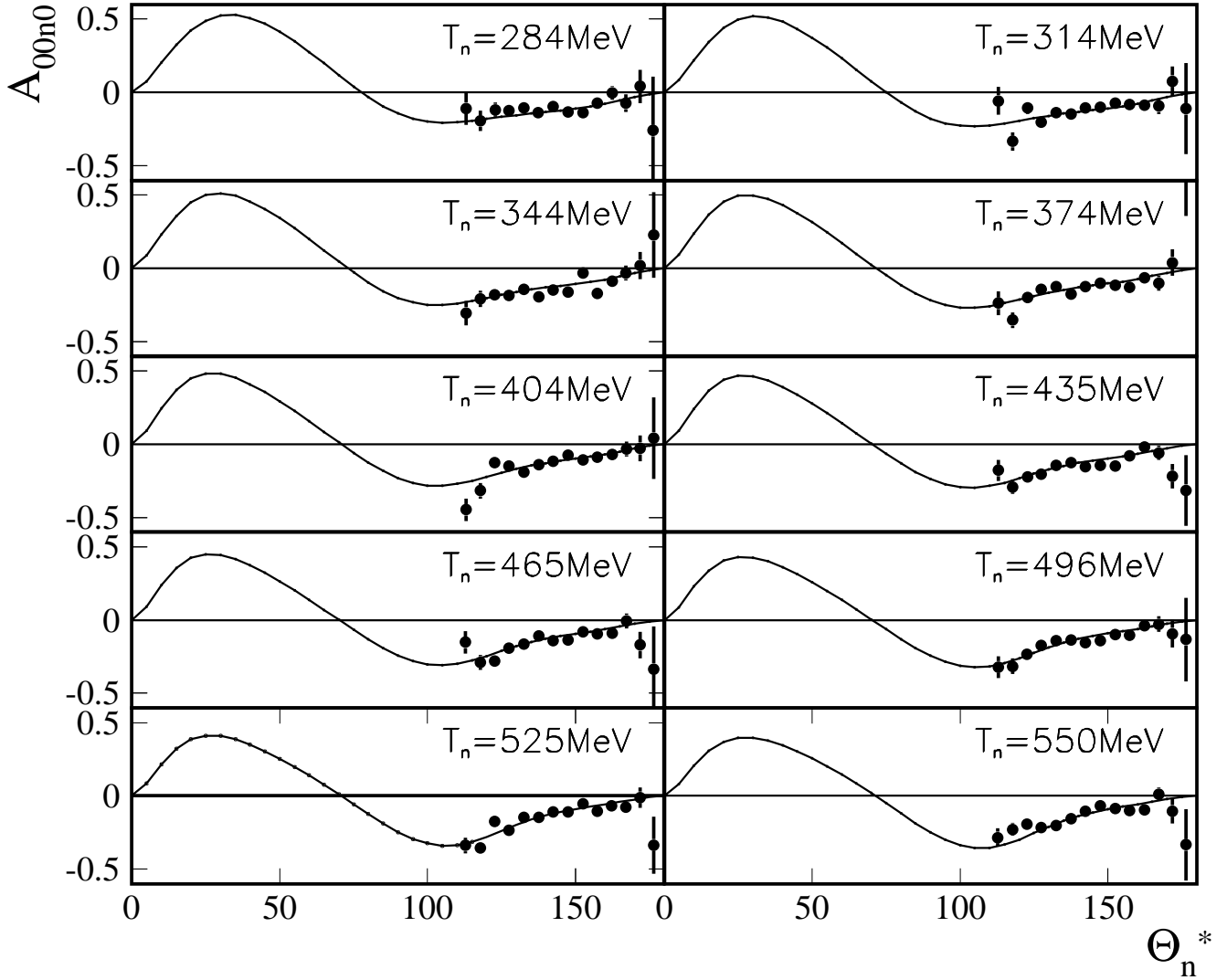


Fig. 1. np elastic scattering: analysing powers A_{00n0} as a function of the neutron c.m. scattering angle θ_n^* (full dots). Shown are statistical errors only. Solid line: results from the partial wave analysis of Arndt et al. [28] where the new data have not been included.

important. Above 465 MeV, they even surpass the statistical error in certain regions of θ_n^* . The systematic error contains various contributions:

1. An uncertainty of $\pm 3\%$ due to the experimental error in the beam polarisation.
2. The asymmetry from background events produced in the target surroundings. Its effect was determined using data taken with an empty target cell. However, the statistical precision was significantly smaller than for the data with the full target cell. For energies above 400 MeV, the asymmetries from this background were found to have the same sign as the asymmetries with the full target cell. However, they were smaller in magnitude by about a factor of two. According to the background contribution, between 4% at 550 MeV and 6% at 400 MeV, the asymmetries were enlarged in magnitude by 2% to 3%, respectively. For energies below

400 MeV, the background asymmetries were consistent with zero on average. The background contribution in the data with full target cell increases with decreasing energy and reads 8% at 315 MeV. As a consequence, the asymmetry was corrected by the same size. Since the statistical error for the empty target measurement is quite large, an additional systematic error of the size of the correction was assigned.

3. If the velocities of the three emitted particles are similar, the kinematical fit procedure possibly assigns the wrong particle hypothesis to the measured tracks [2]. From a conservative estimate, using the detector Monte Carlo simulation, it was concluded that this happens in less than 5% of the events. This effect could lead to a bias by reducing the measured asymmetry. It was taken into account by increasing the value of A_{N0} by

$\pm 2.5\%$ and assigning an additional systematic error of the same size.

The various systematic errors have been added in quadrature.

The numerical results for $A_{N0}(\cos\theta_\pi^*)$ are presented in Tab. 2. In general, large negative values for the analysing powers $A_{N0}(\cos\theta_\pi^*)$ are observed, as can be seen in Fig. 2. At 315 MeV, values compatible with zero are found in the forward and backward direction, whereas negative values are observed around $\cos\theta_\pi^* \approx 0$. At 345 MeV, a positive value, though consistent with zero, is found in the backward direction. At intermediate energies, the angular dependence of A_{N0} is more or less forward-backward symmetric whereas at higher energies a significant forward-backward asymmetry is observed.

The results for the analysing powers $A_{S0}(\cos\theta_\pi^*)$ are shown in Fig. 3. Averaging the $A_{S0}(\cos\theta_\pi^*)$ over $\cos\theta_\pi^*$, the maximal deviation from zero is found to be 1.1 standard deviations. The asymmetries, averaged over θ_π^* , show the smallest statistical errors at $T_n = 525$ MeV. They read

$$\langle \epsilon_S \rangle = \langle P \rangle \cdot \langle A_{S0} \rangle = 0.0007 \pm 0.0014$$

and

$$\langle \epsilon_N \rangle = \langle P \rangle \cdot \langle A_{N0} \rangle = -0.1024 \pm 0.0014.$$

Hence, the $A_{S0}(\cos\theta_\pi^*)$ -values are consistent with zero, which is in agreement with the result observed in the elastic np scattering case. As a consequence, also for the three-body final state, no significant bias from detector asymmetries or beam properties is observed within the available statistical precision.

4.3 Comparison with other experiments

4.3.1 Proton-Proton experiments

In an experiment described in Ref. [21], analysing powers for the reaction $pp \rightarrow pp\pi^0$ have been measured and found to be negative for all beam energies between 319 MeV and 496 MeV. However, these results were presented in the laboratory system only. Due to the different experimental set-ups, they can not be directly compared to our data.

In a SATURNE experiment, analysing powers from the reaction $pp \rightarrow pp\pi^0$ have been measured at various proton beam energies between 325 MeV and 1012 MeV [20].

Although these data do not cover the full angular range for all beam energies, they suggest to be forward-backward symmetric. The negative values, observed for energies above 460 MeV, were interpreted as an interference between P_s and P_p partial waves from σ_{11} [20].

For high energies (above 460 MeV), the asymmetries of Ref. [20], shown in Fig. 2 as boxes, differ in the forward direction ($\cos\theta_\pi^* \approx 0.5$) in a significant way from those measured in $np \rightarrow pp\pi^-$. This is a clear signal that σ_{01} is present in the reaction $np \rightarrow pp\pi^-$. The difference is observed at high energies where the pion production mechanism for σ_{11} is already dominated by the excitation of

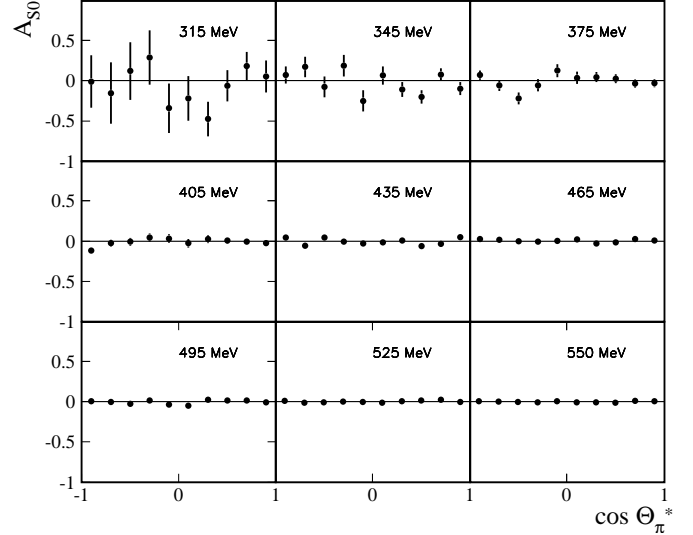


Fig. 3. Analysing powers A_{S0} as a function $\cos\theta_\pi^*$.

an intermediate $N\Delta$ state. Hence, σ_{01} is still of importance for $np \rightarrow pp\pi^-$ even at energies where resonant pion production dominates. This qualitative finding is in agreement with the result from ref. [2] where in the same energy region a 20 – 30 % contribution of σ_{01} to the total $np \rightarrow pp\pi^-$ cross section has been reported.

The asymmetries from Ref. [20] at $T_p = 325$ MeV are slightly positive and differ at $\cos\theta_\pi^* \approx 0$ from our $np \rightarrow pp\pi^-$ results though our uncertainties are large. Measurements performed at the Indiana Cooler synchrotron gave negative asymmetries in the reaction $pp \rightarrow pp\pi^0$ for all proton beam energies between $T_p = 325$ MeV and 400 MeV [30]. Their results are shown in Fig. 2 as open circles. Again, for $T_p = 325$ MeV, their results differ from $np \rightarrow pp\pi^-$ around $\cos\theta_\pi^* \approx 0$. For proton energies at 350 MeV and 375 MeV, the statistical accuracy in the $np \rightarrow pp\pi^-$ results still does not allow to state significant differences between both reactions. However, at 400 MeV the analysing power reported in Ref. [30] clearly differs from the $np \rightarrow pp\pi^-$ data.

4.3.2 Neutron-Proton experiments

In a TRIUMF experiment, analysing powers $A_{N0}(\cos\theta_\pi^*)$ were measured [12] at 443 MeV and presented in different bins of M_{pp} . At 435 MeV, we calculated $A_{N0}(\cos\theta_\pi^*)$ for the same M_{pp} binning as in Ref. [12]. The numerical values are given in Tab. 3. Overall, both data sets are in good agreement as can be seen from Fig. 4. In general, the analysing powers are negative with a slight forward-backward asymmetry. For the smallest M_{pp} bin, both experiments observe a zero-crossing in the backward direction. This finding was interpreted as the sign of an interference between S_s and S_p partial waves [12] and hence as an indication for σ_{01} . This interpretation was confirmed by the results of the TRIUMF experiments described in refs. [16,17].

T_n (MeV)	$\cos \theta_\pi^*$	A_{N0}	σ_{stat}	σ_{sys}	events	T_n (MeV)	$\cos \theta_\pi^*$	A_{N0}	σ_{stat}	σ_{sys}	events
315	-0.9	-0.212	0.323	0.017	262	465	-0.9	-0.217	0.019	0.010	36673
	-0.7	-0.255	0.379	0.021	190		-0.7	-0.370	0.022	0.017	28701
	-0.5	-0.427	0.357	0.034	213		-0.5	-0.472	0.024	0.022	24202
	-0.3	-0.214	0.338	0.017	240		-0.3	-0.475	0.026	0.022	20316
	-0.1	-1.088	0.299	0.097	293		-0.1	-0.411	0.028	0.019	17192
	0.1	-0.910	0.271	0.073	359		0.1	-0.383	0.029	0.018	16083
	0.3	0.218	0.214	0.018	597		0.3	-0.325	0.027	0.015	19361
	0.5	-0.378	0.194	0.030	723		0.5	-0.248	0.024	0.012	23348
	0.7	0.043	0.176	0.003	887		0.7	-0.171	0.023	0.008	26464
0.9	0.427	0.197	0.034	700	0.9	-0.029	0.022	0.001	27803		
345	-0.9	0.188	0.106	0.014	1735	495	-0.9	-0.217	0.015	0.009	76544
	-0.7	-0.037	0.125	0.003	1246		-0.7	-0.382	0.017	0.016	59106
	-0.5	-0.342	0.129	0.025	1165		-0.5	-0.412	0.019	0.017	49809
	-0.3	-0.374	0.135	0.027	1065		-0.3	-0.437	0.020	0.018	41635
	-0.1	-0.405	0.131	0.030	1119		-0.1	-0.429	0.022	0.018	34785
	0.1	-0.230	0.115	0.017	1485		0.1	-0.362	0.023	0.015	31131
	0.3	-0.239	0.093	0.018	2227		0.3	-0.271	0.022	0.011	37177
	0.5	-0.244	0.084	0.018	2790		0.5	-0.194	0.020	0.008	43431
	0.7	-0.189	0.075	0.014	3471		0.7	-0.148	0.018	0.006	50670
0.9	-0.050	0.080	0.004	3072	0.9	-0.031	0.018	0.001	54861		
375	-0.9	-0.051	0.058	0.003	5195	525	-0.9	-0.232	0.008	0.010	178779
	-0.7	-0.189	0.068	0.013	3785		-0.7	-0.407	0.010	0.017	135787
	-0.5	-0.264	0.074	0.017	3175		-0.5	-0.439	0.012	0.018	114000
	-0.3	-0.261	0.077	0.017	2937		-0.3	-0.423	0.012	0.018	93306
	-0.1	-0.425	0.079	0.028	2716		-0.1	-0.359	0.013	0.015	75911
	0.1	-0.378	0.075	0.025	3075		0.1	-0.303	0.014	0.013	66249
	0.3	-0.493	0.063	0.033	4261		0.3	-0.222	0.013	0.009	77681
	0.5	-0.262	0.056	0.017	5568		0.5	-0.174	0.012	0.007	90419
	0.7	-0.115	0.051	0.008	6595		0.7	-0.106	0.011	0.004	105369
0.9	-0.100	0.052	0.007	6335	0.9	-0.044	0.010	0.002	116920		
405	-0.9	-0.113	0.039	0.005	10287	550	-0.9	-0.270	0.008	0.011	157751
	-0.7	-0.217	0.044	0.010	7954		-0.7	-0.416	0.010	0.017	120750
	-0.5	-0.454	0.047	0.021	6743		-0.5	-0.448	0.010	0.019	101710
	-0.3	-0.437	0.051	0.020	5888		-0.3	-0.438	0.012	0.018	82258
	-0.1	-0.480	0.053	0.022	5366		-0.1	-0.381	0.013	0.016	66408
	0.1	-0.464	0.053	0.022	5399		0.1	-0.315	0.014	0.013	57700
	0.3	-0.360	0.047	0.017	6941		0.3	-0.209	0.013	0.009	67116
	0.5	-0.273	0.041	0.013	8939		0.5	-0.140	0.012	0.006	77921
	0.7	-0.231	0.039	0.011	10263		0.7	-0.060	0.011	0.003	89622
0.9	-0.069	0.039	0.003	10196	0.9	-0.021	0.010	0.001	105223		
435	-0.9	-0.126	0.025	0.006	19302						
	-0.7	-0.355	0.029	0.017	14855						
	-0.5	-0.341	0.031	0.016	12846						
	-0.3	-0.488	0.033	0.023	11090						
	-0.1	-0.462	0.036	0.022	9484						
	0.1	-0.418	0.036	0.019	9232						
	0.3	-0.302	0.033	0.014	11421						
	0.5	-0.182	0.029	0.009	13841						
	0.7	-0.095	0.028	0.004	15962						
0.9	-0.086	0.028	0.004	16256							

Table 2. Analysing powers A_{N0} for the reaction $np \rightarrow pp\pi^-$. Quoted are statistical and systematic errors.

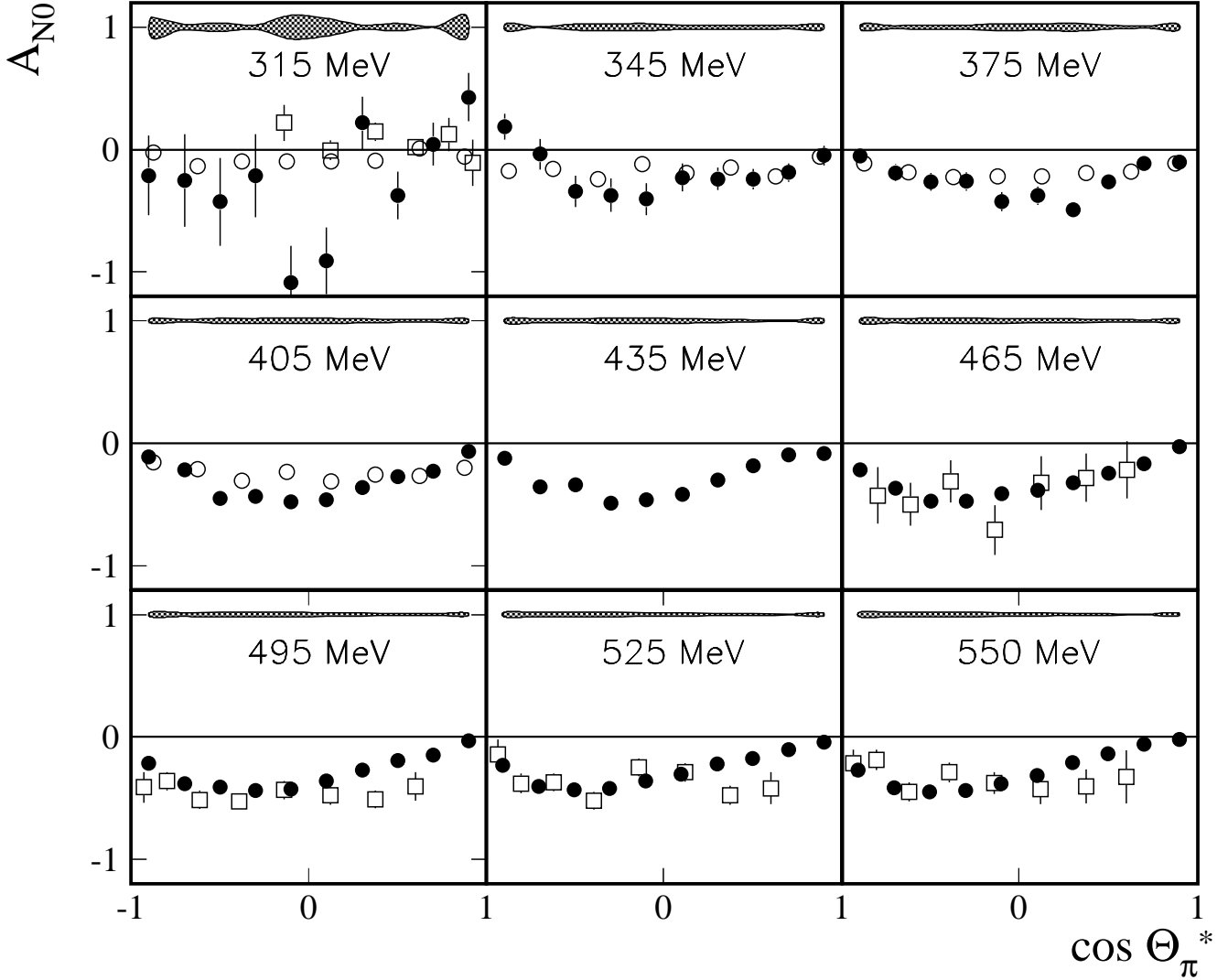


Fig. 2. Analysing powers A_{N0} for the nine bins in neutron energy as a function of $\cos\theta_\pi^*$ (●). The statistical errors are indicated by the error bars. The systematic error is indicated by the shaded band. Also shown are data for the reaction $pp \rightarrow pp\pi^0$ from two experiments: for proton energies $T_p = 325, 460, 500, 520$ and 540 MeV from Ref. [20](□) and for proton energies $T_p = 325, 350, 375, 400$ MeV from Ref. [30](○).

In a SATURNE experiment [15], analysing powers $A_{N0}(\theta_\pi^*)$ were measured in different bins of M_{pp} at several neutron energies. The lowest neutron beam energy which can be compared with our results was at 572 MeV. Fig. 5 shows their results as a function of $\cos\theta_\pi^*$ together with our $A_{N0}(\cos\theta_\pi^*)$ values at 550 MeV using the same M_{pp} binning. The numerical values are given in Tab. 4. Both experiments are in qualitative agreement. Quantitative deviations might be assigned to the difference in the beam energies. In both cases, the analysing powers are mainly negative. Compared to the results at 435 MeV, see Fig. 4, the forward-backward asymmetry is even more pronounced. Again, for the smallest M_{pp} bin, a zero-crossing is observed; however, this time in the forward direction.

4.4 Results for small invariant proton-proton masses

Since the zero-crossing in the forward direction at 550 MeV in Fig. 5 is observed in the lowest M_{pp} regime only, the observed pattern is likely due to an interference between various partial waves with a $pp(^1S_0)$ final state. To study this effect in more detail, analysing powers were determined by selecting events with small M_{pp} values. Since the reconstruction efficiency drops at small M_{pp} , a loose cut, $M_{pp} - 2 \cdot M_p < 6$ MeV, was chosen in order to collect sufficient statistics. As a consequence, there is a significant dilution due to partial waves with the two protons being in a relative P-wave. Therefore, the results can be used only for a qualitative discussion.

The $A_{N0}(\theta_\pi^*)$ -values for the small M_{pp} cut are shown in Fig. 6. Despite the loose M_{pp} cut there is only small

M_{pp} (MeV)	$\cos \theta_\pi^*$	A_{N0}	σ_{stat}	σ_{sys}	events	M_{pp} (MeV)	$\cos \theta_\pi^*$	A_{N0}	σ_{stat}	σ_{sys}	events
1876-1888	-0.9	0.361	0.084	0.018	1749	1912-1924	-0.9	-0.239	0.053	0.012	4511
	-0.7	-0.092	0.116	0.005	934		-0.7	-0.388	0.057	0.019	3845
	-0.5	-0.075	0.137	0.004	668		-0.5	-0.338	0.061	0.017	3358
	-0.3	-0.031	0.146	0.002	589		-0.3	-0.478	0.067	0.024	2729
	-0.1	-0.446	0.136	0.022	663		-0.1	-0.442	0.077	0.022	2060
	0.1	-0.495	0.125	0.024	785		0.1	-0.471	0.077	0.023	2041
	0.3	-0.073	0.095	0.004	1378		0.3	-0.330	0.073	0.016	2330
	0.5	-0.074	0.072	0.004	2386		0.5	-0.217	0.073	0.011	2359
	0.7	0.083	0.063	0.004	3197		0.7	-0.210	0.071	0.010	2487
0.9	0.004	0.064	0.000	3033	0.9	-0.144	0.069	0.007	2606		
1888-1900	-0.9	-0.193	0.050	0.009	4945	1924-1936	-0.9	-0.280	0.076	0.014	2150
	-0.7	-0.299	0.060	0.015	3458		-0.7	-0.531	0.084	0.026	1724
	-0.5	-0.379	0.064	0.019	3034		-0.5	-0.343	0.094	0.017	1383
	-0.3	-0.515	0.067	0.025	2672		-0.3	-0.693	0.107	0.034	1038
	-0.1	-0.444	0.070	0.022	2470		-0.1	-0.572	0.118	0.028	873
	0.1	-0.369	0.073	0.018	2287		0.1	-0.397	0.114	0.020	947
	0.3	-0.430	0.064	0.021	3024		0.3	-0.169	0.113	0.008	974
	0.5	-0.126	0.056	0.006	4052		0.5	-0.393	0.115	0.019	922
	0.7	-0.123	0.051	0.006	4861		0.7	-0.196	0.109	0.010	1041
0.9	-0.020	0.051	0.001	4841	0.9	-0.208	0.100	0.010	1248		
1900-1912	-0.9	-0.312	0.047	0.015	5603	1936-1948	-0.9	-0.070	0.192	0.003	338
	-0.7	-0.425	0.051	0.021	4663		-0.7	-0.422	0.232	0.021	227
	-0.5	-0.408	0.054	0.020	4211		-0.5	-0.597	0.252	0.029	189
	-0.3	-0.501	0.056	0.025	3862		-0.3	-0.514	0.248	0.025	198
	-0.1	-0.534	0.062	0.026	3193		-0.1	-0.083	0.240	0.004	216
	0.1	-0.436	0.064	0.022	2979		0.1	-0.162	0.258	0.008	187
	0.3	-0.406	0.059	0.020	3511		0.3	-0.229	0.252	0.011	196
	0.5	-0.196	0.056	0.010	3911		0.5	-0.175	0.245	0.009	207
	0.7	-0.092	0.055	0.005	4141		0.7	-0.068	0.232	0.003	232
0.9	-0.167	0.054	0.008	4255	0.9	-0.053	0.214	0.003	272		

Table 3. Analysing powers A_{N0} for the reaction $np \rightarrow pp\pi^-$ at $T_n = 435$ MeV for different bins in M_{pp} . Quoted are statistical and systematic errors.

statistics in the backward region since there the differential cross section and the reconstruction efficiency is smaller than in the forward region. Nevertheless, one can state that, in general, positive analysing powers are observed in the backward region and negative values around $\cos \theta_\pi^* \approx 0$. For beam energies above 405 MeV, positive analysing powers are observed in the forward direction the magnitude of which increases with neutron energy.

Two zero-crossings in $A_{N0}(\theta_\pi^*)$ have already been reported at 440 MeV [17] and are interpreted as a contribution from Sd partial waves. A possible significant contribution from d-wave pions at quite small beam energies was also reported in a CELSIUS experiment measuring the reaction $pp \rightarrow pp\pi^0$ [29].

Given this, our data imply a relative increase of Sd partial waves as a function of beam energy. Such a behaviour fits the naive expectation for the energy dependence of partial waves. For a $pp(^1S_0)$ final state, the excitation function is supposed to scale like $\eta^{2-(\ell+1)}$, see, *e.g.*, Ref. [2]. Therefore, the contribution of d-wave pions should increase relative to s- or p-wave pions as the neutron energy increases. It should be noted however that this is only a qualitative argument. On one hand, the matrix element close to threshold shows a strong energy dependence in the pp-interaction part [18]. On the other hand, at very high en-

ergies, the momenta of the outgoing particles are large. As a consequence, the approximation entering this prediction, see, *e.g.*, Ref. [31], is no longer justified. Moreover, a dynamical suppression of the Ss partial wave is predicted in meson production models.

5 Conclusion

The results of the analysing power A_{N0} in the reaction $np \rightarrow pp\pi^-$ were presented as a function of the pion c.m. angle θ_π^* in different bins of the proton-proton invariant mass M_{pp} for neutron energies from threshold up to 570 MeV. Except for two experiments at 443 MeV [12] and 572 MeV [15], these are the first measurements of this observable over the full phase space and below the two-pion production threshold. The comparison with the reaction $pp \rightarrow pp\pi^0$ clearly shows the presence of σ_{01} in the reaction $np \rightarrow pp\pi^-$. The results obtained for small M_{pp} indicate a significant contribution from Sd partial waves at large neutron energies.

The additional knowledge from these spin dependent observables provides important information to disentangle the contributions from different partial waves. Such a partial wave analysis should be performed by combining data

M_{pp} (MeV)	$\cos \theta_\pi^*$	A_{N0}	σ_{stat}	σ_{sys}	events	M_{pp} (MeV)	$\cos \theta_\pi^*$	A_{N0}	σ_{stat}	σ_{sys}	events
1876-1902	-0.9	-0.109	0.023	0.005	24525	1952-1977	-0.9	-0.301	0.027	0.013	16778
	-0.7	-0.222	0.028	0.010	16291		-0.7	-0.446	0.030	0.020	13970
	-0.5	-0.227	0.030	0.010	13512		-0.5	-0.480	0.034	0.021	10644
	-0.3	-0.309	0.021	0.014	11954		-0.3	-0.425	0.041	0.019	7209
	-0.1	-0.261	0.034	0.011	10565		-0.1	-0.411	0.047	0.018	5544
	0.1	-0.228	0.036	0.010	9597		0.1	-0.497	0.046	0.022	5676
	0.3	-0.094	0.031	0.004	13071		0.3	-0.223	0.044	0.010	6290
	0.5	-0.051	0.026	0.002	18860		0.5	-0.223	0.045	0.010	6137
	0.7	0.099	0.022	0.004	25013		0.7	-0.124	0.043	0.005	6809
	0.9	0.040	0.021	0.002	28978		0.9	0.007	0.039	0.000	8123
1902-1927	-0.9	-0.304	0.014	0.013	64098	1977-2000	-0.9	-0.103	0.085	0.005	1736
	-0.7	-0.486	0.016	0.021	48795		-0.7	-0.018	0.104	0.001	1156
	-0.5	-0.490	0.017	0.021	43086		-0.5	-0.472	0.120	0.021	842
	-0.3	-0.459	0.019	0.020	35549		-0.3	-0.400	0.124	0.018	798
	-0.1	-0.383	0.020	0.017	29543		-0.1	-0.514	0.115	0.023	919
	0.1	-0.265	0.022	0.012	24759		0.1	-0.439	0.117	0.019	892
	0.3	-0.203	0.021	0.009	28268		0.3	-0.352	0.118	0.015	889
	0.5	-0.160	0.019	0.007	33350		0.5	-0.122	0.112	0.005	988
	0.7	-0.102	0.018	0.004	37409		0.7	-0.196	0.112	0.000	994
	0.9	0.039	0.017	0.027	43954		0.9	0.026	0.115	0.011	1125
1927-1952	-0.9	-0.345	0.016	0.015	50612						
	-0.7	-0.471	0.017	0.021	40536						
	-0.5	-0.500	0.019	0.022	33626						
	-0.3	-0.494	0.021	0.022	26747						
	-0.1	-0.411	0.025	0.018	19836						
	0.1	-0.328	0.027	0.014	16775						
	0.3	-0.267	0.026	0.012	18598						
	0.5	-0.177	0.026	0.008	18786						
	0.7	-0.113	0.025	0.005	19395						
	0.9	-0.036	0.023	0.002	23043						

Table 4. Analysing powers A_{N0} for the reaction $np \rightarrow pp\pi^-$ at $T_n = 550$ MeV for different bins in M_{pp} . Quoted are statistical and systematic errors.

from both reactions, $np \rightarrow pp\pi^-$ and $pp \rightarrow pp\pi^0$. Recently, such an analysis was performed for the σ_{11} contribution using a complete set of polarisation observables measured in the reaction $pp \rightarrow pp\pi^0$ for proton beam energies between 315 MeV and 400 MeV [30]. As a consequence, the σ_{11} is already quite well known. For the cross section σ_{01} , recent experimental results suggest that the main contribution in this energy region is provided by only two partial waves, ${}^3D_1 \rightarrow {}^1S_0p_1$ and ${}^3S_1 \rightarrow {}^1S_0p_1$ [2] which will facilitate the analysis.

It would be also interesting to confront model calculations for pion production with the new data. However, for the reaction $np \rightarrow pp\pi^-$, except for very small proton-proton invariant masses, there are no published model calculations neither for differential cross sections nor for spin observables in the energy region of interest.

For the elastic np scattering, A_{00n0} was measured in 10 energy bins over the backward hemisphere angular region. The results will improve the existing database for phase shift analyses.

Acknowledgements

We express our gratitude to C. Lechanoine-Leluc, D. Rapin and the DPNC of the University of Geneva for providing us the scintillators for the TOF wall and the associated electronics.

We thank M. Laub and J. Zicha for their help with the construction and the setup of the experiment.

We acknowledge the excellent cooperation with the staff of PSI during the installation and running of the experiment and the analysis as well.

We appreciate the contribution of G. Braun, R. Fastner, H. Fischer and J. Urban.

We thank C. Hanhart for the stimulating discussions.

This work has been funded by the German Bundesministerium für Bildung und Forschung under the contract No. 06FR845.

References

1. A. H. Rosenfeld, Phys. Rev. **96**, 139 (1954)
2. M. Daum et al., accepted for publication in Eur. Phys. J.; nucl-ex/0108008
3. R. Handler, Phys. Rev. **138**, 1230 (1965)

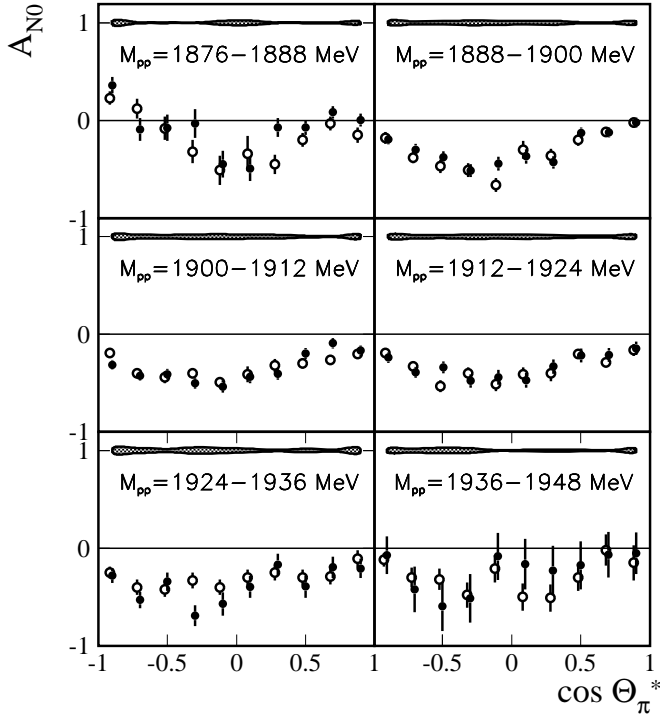


Fig. 4. Comparison of $A_{N0}(\cos\theta_{\pi}^*)$ values (\bullet) at 435 MeV subdivided in different bins of M_{pp} with the results of Ref. [12] at 443 MeV (\circ).

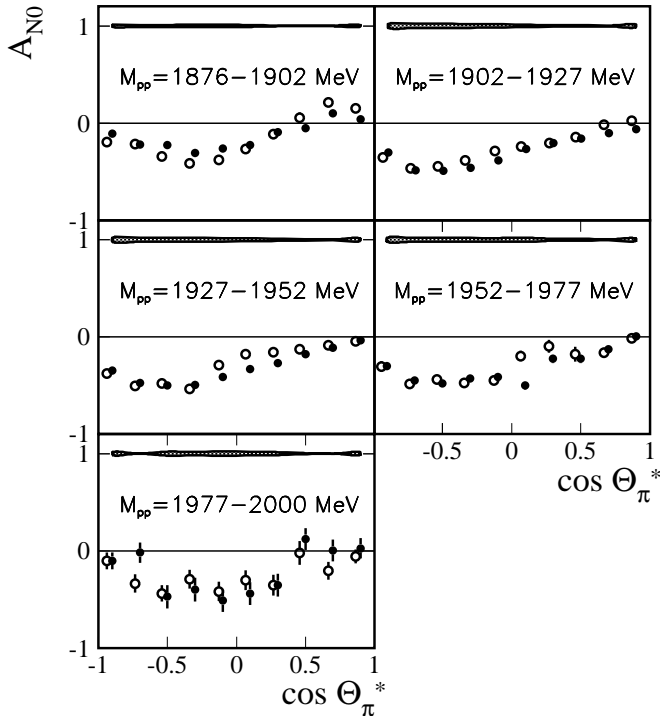


Fig. 5. Comparison of $A_{N0}(\cos\theta_{\pi}^*)$ values (\bullet) at 550 MeV subdivided in different bins of M_{pp} with the results of Ref. [15] at 572 MeV (\circ).

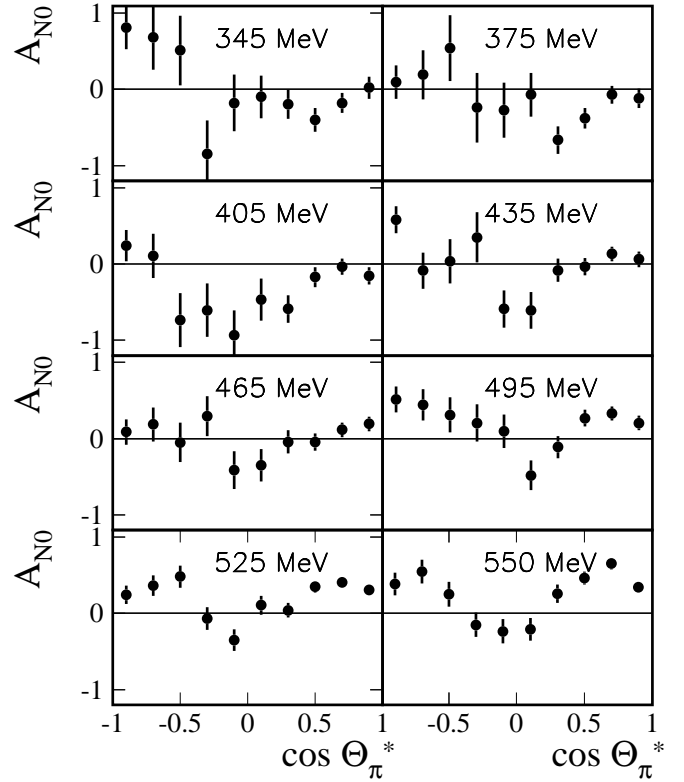


Fig. 6. Analysing powers $A_{N0}(\theta_{\pi}^*)$ for small proton-proton invariant masses $M_{pp} - 2M_p < 6$ MeV.

4. J. G. Rushbrooke et al., *Nuovo Cimento* **33**, 1509 (1964)
5. V. D. Dzhelepov et al., *Sov. Phys. JETP* **23**, 993 (1966)
6. M. Kleinschmidt et al., *Z. Phys.* **A298**, 253 (1980)
7. W. Thomas et al., *Phys. Rev.* **D24**, 1736 (1981)
8. L. G. Dakhno et al., *Phys. Lett.* **B114**, 409 (1982)
9. T. Tsuboyama et al., *Nucl. Phys.* **A486**, 669 (1988)
10. Yu. M. Kazarinov and Yu. N. Simonov, *Sov. Jour. Nucl. Phys.* **4**, 100 (1967)
11. A. Bannwarth et al., *Nucl. Phys.* **A567**, 761 (1994)
12. M. G. Bachman et al., *Phys. Rev.* **C52**, 495 (1995)
13. B. J. VerWest and R. A. Arndt, *Phys. Rev.* **C25**, 1979 (1982)
14. J. Bystricky et al., *J. Physique* **48**, 1901 (1987)
15. Y. Terrien et al., *Phys. Lett.* **B294**, 40 (1992)
16. F. Duncan et al., *Phys. Rev. Lett.* **80**, 4390 (1998)
17. H. Hahn et al., *Phys. Rev. Lett.* **82**, 2258 (1999)
18. H. O. Meyer et al., *Phys. Rev. Lett.* **65**, 2846 (1990)
19. A. Bondar et al., *Phys. Lett* **B356**, 8 (1995)
20. G. Rappenecker et al., *Nucl. Phys.* **A590**, 763 (1995)
21. S. Stanislaus et al., *Phys. Rev* **C44**, 2287 (1991)
22. A. F. Dunaitsev and Yu. D. Prokoshkin, *Sov. Phys. JETP* **9**, 1179 (1959)
23. H. Lacker, Dissertation, University of Freiburg (2000)
24. J. Arnold et al., *Nucl. Instr. & Meth.* **A386**, 211 (1997)
25. J. Arnold et al., *Eur. Phys. J.* **A2**, 411 (1998)
26. D. Besset et al., *Nucl. Instr. & Meth.* **166**, 515 (1979)
27. J. Bystricky, F. Lehar and P. Winternitz, *J. Physique* **1**, 1 (1978)
28. R. A. Arndt et al., *Phys. Rev.* **D45**, 3995 (1992); actual solution 2000

29. J. Zlomanczuk et al., The Svedberg Laboratory (TSL) and Department of Radiation Sciences at Uppsala University, TSL/ISV-98-0196, (1998)
30. H.O. Meyer et al., Phys.Rev. **C63**, 064002 (2001)
31. C. Hanhart, Dissertation, University of Bonn (1997)
32. J. A. Niskanen, Phys. Lett. **B289**, 227 (1992); Phys. Rev. **C49**, 1285 (1994)